Colloids and Surfaces B: Biointerfaces 112 (2013) 74–80

Contents lists available at ScienceDirect

Colloids and Surfaces B: Biointerfaces

journal homepage: www.elsevier.com/locate/colsurfb

A novel promising biomolecule immobilization matrix: Synthesis of functional benzimidazole containing conducting polymer and its biosensor applications

Sema Demirci Uzun[a], Naime Akbasoglu Unlu[b], Merve Sendur[c], Fulya Ekiz Kanik[d], Suna Timur[e], Levent Toppare[a,b,d,f,*]

[a] Department of Polymer Science and Technology, Middle East Technical University, 06800 Ankara, Turkey
[b] Department of Chemistry, Middle East Technical University, 06800 Ankara, Turkey
[c] Institut für Physikalische und Theoretische Chemie, Universität Regensburg, 93053 Regensburg, Germany
[d] Department of Biotechnology, Middle East Technical University, 06800 Ankara, Turkey
[e] Department of Biochemistry, Faculty of Science, Ege University, 35100 Bornova-Izmir, Turkey
[f] The Center for Solar Energy Research (GÜNAM), Middle East Technical University, 06800 Ankara, Turkey

ARTICLE INFO

Article history:
Received 19 June 2013
Received in revised form 26 July 2013
Accepted 28 July 2013
Available online 2 August 2013

Keywords:
Conducting polymer
Biosensor
Enzyme immobilization
Low detection limit
Glucose level

ABSTRACT

In order to construct a robust covalent binding between biomolecule and immobilization platform in biosensor preparation, a novel functional monomer 4-(4,7-di(thiophen-2-yl)-1*H*-benzo[*d*]imidazol-2-yl)benzaldehyde (BIBA) was designed and successfully synthesized. After electropolymerization of this monomer, electrochemical and spectroelectrochemical properties were investigated in detail. To fabricate the desired biosensor, glucose oxidase (GOx) was immobilized as a model enzyme on the polymer coated graphite electrode with the help of glutaraldehyde (GA). During the immobilization step, an imine bond was formed between the free amino groups of enzyme and aldehyde group of polymer. The surface characterization and morphology were investigated to confirm bioconjugation by X-ray photoelectron spectroscopy (XPS) and transmission electron microscopy (TEM) at each step of biosensor fabrication. The optimized biosensor shows good linearity between 0.02 mM and 1.20 mM and a low limit of detection (LOD) of 2.29 μM. Kinetic parameters K_m^{app} and I_{max} were determined as 0.94 mM and 10.91 μA, respectively. The biosensor was tested for human blood serum samples.

1. Introduction

Conducting polymers (CPs) with their fascinating electronic, electrochemical and optical properties have crucial contribution to material science. Conjugated polymers have high electron affinity, low ionization potential, low energy for optical transitions which makes them useful materials for technological developments [1]. Thus, these multifunctional materials have the wide range of promising applications in the fields of energy storage [2,3], electrocatalysis [4,5], electrochromic devices [6,7], sensors [8,9] and molecular electronic devices [10,11].

Integration of biomolecules such as enzymes, antibodies and amino acids with CPs provides improvement of many electrochemical, electronic and optical biosensors [12,13]. A biosensor mainly consists of a biological recognition element and a transducer which transforms the signal resulting from reaction between biomolecule and its analyte into a measurable signal. The most significant challenge for the construction of a biosensor is to achieve a robust attachment between transducer and protein molecule. Among well-known immobilization techniques, covalent binding is remarkably powerful method for bioconjugation [14]. This easily applicable technique allows fabricating new generation biosensors with high activity, stability, sensitivity and faster response time in detection [15]. Since enzymes are huge molecules, immobilization platform should be well organized to promote interaction with biomolecule. Increase in the functional groups on the surface provides the maximum enzyme loading with high stability. For this purpose, functionalized conducting polymers are favorable materials and can be used as conjugation matrices for biomolecules [16]. Since polybenzimidazoles are biocompatible molecules and widely used in biological applications, aldehyde functionalized donor acceptor donor type benzimidazole containing polymer was utilized as a bioconjugation platform in this study [17].

* Corresponding author at: Middle East Technical University, Department of Chemistry, 06800 Ankara, Turkey. Tel.: +90 3122103251; fax: +90 3122103200.
E-mail addresses: demircisema@gmail.com (S.D. Uzun), naimeakbasoglu@gmail.com (N.A. Unlu), mervesen@gmail.com (M. Sendur), fulyaekiz@gmail.com (F.E. Kanik), suna.timur@ege.edu.tr (S. Timur), toppare@metu.edu.tr (L. Toppare).

0927-7765/$ – see front matter © 2013 Elsevier B.V. All rights reserved.
http://dx.doi.org/10.1016/j.colsurfb.2013.07.049

Glucose oxidase (GOx) has high resistance against unfavorable microenvironment conditions such as acidic media and denaturing agents. Since it is also commercially available with low price and has two flavine adenine dinucleotide (FAD) units, this enzyme is widely used in many analytical detection studies [18,19]. During the detection of glucose, β-D-glucose is oxidized to gluconolactone by GOx and gluconolactone is hydrolyzed to gluconic acid. As a second step, reduced GOx is reoxidized in the presence of molecular oxygen [20]. In amperometric studies, consumption of oxygen or formation of H_2O_2 resulting from reduction of oxygen are monitored.

In this report, we highlight design and synthesis of a novel functionalized conducting polymer for biomolecule immobilization. In this context, the electronic and optoelectronic properties of this polymer were examined in detail. To investigate the biological matrix properties of this system, firstly, corresponding monomer was electropolymerized on graphite electrode. Then, GOx as a model enzyme was covalently immobilized on the polymer coated electrode. Meanwhile, imine bonds were achieved between free amine groups of enzyme and aldehyde groups of polymer structure. Furthermore, glutaraldehyde was used as the crosslinking agent providing a compact structure for enzyme on electrode surface. Thus, bioconjugation was successfully performed with the formation of desired robust binding. The new biosensor was optimized for parameters like scan number in polymerization, amount of loaded enzyme, glutaraldehyde amount and pH of the buffer solution used in the amperometric measurements. Optimum biosensor was characterized in terms of kinetic parameters, K_M^{app} and $I_{max.}$ During the detection of glucose, amperometric studies were carried out at −0.7 V to monitor the consumption of molecular oxygen. Surface morphology and characteristic were explored via TEM and XPS. Finally, accuracy of fabricated biosensor was tested for glucose amount in human blood serum samples.

2. Materials and methods

2.1. Materials

All chemicals used in monomer synthesis were commercially obtained and used without any purification. THF was distilled over sodium and benzophenone. 4-(4,7-Dibromo-1*H*-benzo[*d*]imidazol-2-yl)benzaldehyde, 4-(4,7-di(thiophen-2-yl)-1*H*-benzo[*d*]imidazol-2-yl)benzaldehyde and tributyl(thiophene-2-yl)stannane were synthesized. All chemicals used in the synthesis of the monomer (bromine, bromic acid, dichloromethane (DCM)) were purchased from Sigma except for thiophene which was purchased from Acros Organics (Geel, Belgium). Glucose oxidase (GOx, β-D-glucose: oxygen 1-oxidoreductase, EC 1.1.3.4, 21 200 units/g) from *Aspergillus niger*, D-glucose, sodiumborohydride were purchased from Sigma (St. Louis, USA). Acetonitrile, hydrochloric acid, sodium hydroxide were purchased from Merck (Darmstadt, Germany). All chemicals used for electropolymerization were purchased from Aldrich. All other chemicals were analytical grade. Real human serum samples were obtained from Middle East Technical University (METU) Medical Center from patients volunteered for that matter.

2.2. Apparatus

All experiments were carried out in pre-dried glassware (1 h, 150 °C) under argon atmosphere. ^{1}H NMR and ^{13}C NMR spectra were recorded in DMSO-d_6 on Bruker Spectrospin Avance DPX-400 spectrometer and the chemical shifts were expressed in ppm relative to DMSO-d_6 (d 2.50 and 39.52 for ^{1}H and ^{13}C NMR, respectively) as the internal standard. Amperometric and cyclic voltammetry measurements were carried out using Palm Instrument (PalmSens, Houten, The Netherlands, www.palmsens.com) with a conventional three electrode configuration. As the working electrode, graphite electrodes (Ringsdorff Werke GmbH, Bonn, Germany, type RW001, 3.05 mm diameter and 13% porosity) were used. Ag/AgCl (3 M KCl saturated with AgCl) and a Pt electrode (Metrohm, Switzerland, www.metrohm.com) were used as the reference and counter electrodes, respectively. XPS (X-ray Photoelectron Spectroscopy) was carried out on a PHI 5000 Versa Probe (*Φ* ULVAC-PHI, Inc., Japan/USA) model X-ray photoelectron spectrometer instrument with monochromatized Al Kα radiation (1486.6 eV) as an X-ray anode at 24.9 W. The pressure inside the analyzer was maintained at 10^{-7} Pa. The binding energy scale was referenced by setting the C—H peak maximum in the C 1s spectrum to 285.0 eV and the atomic composition was estimated using Multipak software. Transmission electron microscope (CTEM) images were recorded using FEI Tecnai G^2 Spirit BioTwin CTEM Microscope.

3. Experimental

3.1. Synthesis of the monomer

3.1.1. Synthesis of 4-(4,7-dibromo-1H-benzo[d]imidazol-2-yl) benzaldehyde

3,6-Dibromobenzene-1,2-diamine was synthesized as reported in literature [21]. After the bromination of 2,1,3-benzothiadiazole in the presence of HBr/Br_2, reduction of 4,7-dibromobenzo[*c*][1,2,5]thiadiazole was performed with $NaBH_4$ in ethanol. 3,6-Dibromobenzene-1,2-diamine (8.50 mmol, 2.30 g), terephthalaldehyde (34 mmol, 4.56 g) and $ZrCl_4$ (0.43 mmol, 97.75 mg) were dissolved in acetonitrile (ACN) (150 mL) and the mixture was stirred at room temperature for 24 h. After the solid product was filtered, 150 mL ACN was added and the mixture was heated overnight under reflux conditions [22]. Afterwards the purified product was filtered as a pale yellow solid (5.1 mmol, 1.53 g, 60%). ^{1}H NMR (d-DMSO): δ 10.10 (s, 1H), 8.56 (d, 2H, J = 8.26 Hz), 8.10 (d, 2H, J = 8.36 Hz), 7.43 (s, 2H). ^{13}C NMR (d-DMSO): 1927. 1517. 1 37 1.1 34.1. 1298. 1280. 1268, 1267, 126.6.

3.1.2. Synthesis of 4-(4,7-di(thiophen-2-yl)-1H-benzo[d]imidazol-2-yl)benzaldehyde

Tributyl(thiophene-2-yl)stannane was synthesized according to a previously described method [23]. 4-(4,7-Dibromo-1*H*-benzo[*d*]imidazol-2-yl)benzaldehyde (0.70 g, 1.70 mmol) and tributyl(thiophen-2-yl)stannane (3.18 g, 8.50 mmol) were dissolved in anhydrous THF (50 mL) and dichlorobis(triphenylphosphine)-palladium(II) (50 mg, 0.05 mmol) was added at room temperature. The mixture was refluxed for 12 h under argon atmosphere. Solvent was evaporated under vacuum and the crude product was purified by silica gel column chromatography as a yellow solid. (eluent: DCM) (0.60 g, 45%). ^{1}H NMR (d-DMSO): δ 12.89 (s, 1H), 10.12 (s, 1H), 8.62 (d, 2H, J = 8.23 Hz), 8.26 (d, 1H, J = 3.56 Hz), 8.11 (d, 2H, J = 8.22 Hz), 7.72–7.65 (m, 4H), 7.40 (d, 1H, J = 7.85 Hz), 7.28 (dt, 1H, J = 4.74 and 3.91 Hz), 7.25 (dt, 1H, J = 4.76 and 3.91 Hz). ^{13}C NMR (d-DMSO): δ 192.2, 150.8, 140.1, 139.1, 138.4, 136.2, 134.3, 132.3, 129.2, 127.8, 127.5, 127.1, 126.1, 125.8, 125.5, 123.5, 122.8, 118.9, 117.6. HRMS: Calculated $[M]^+$ 387.0626, Measured $[M]^+$ 387.0631.

3.2. Amperometric measurements

All measurements; generation of a calibration curve and determining glucose concentration in samples, were achieved at −0.7 V versus Ag/AgCl electrode in 50 mM sodium acetate buffer, pH 5.5, while mildly stirring the medium at room temperature. Hence, current difference between baseline and steady state (before and after

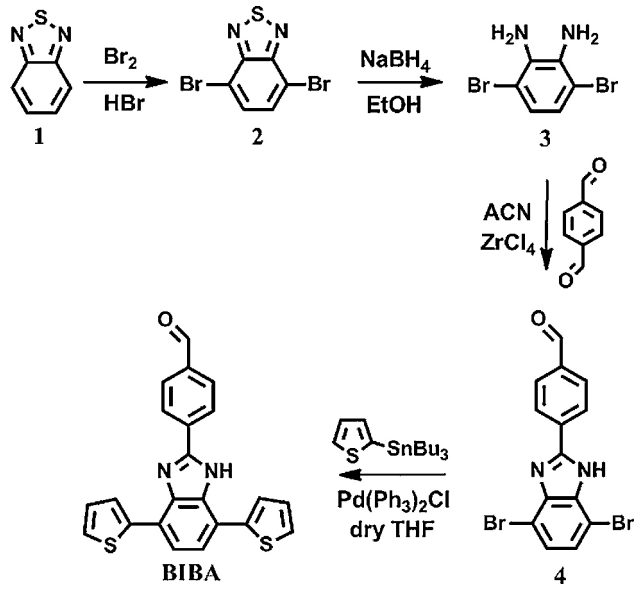

Scheme 1. Synthetic pathway of monomer synthesis.

adding glucose sample to 10 mL sodium acetate buffer in electrochemical cell) was monitored and results were recorded for each glucose concentration. After each measurement, electrodes and cell were washed with distilled water and buffer solution was refreshed before running the next experiment. During the amperometric measurements, average of three current values for each glucose concentration was recorded and standard deviations were calculated as ±SD.

4. Results and discussion

4.1. Synthesis of designed monomer

The synthetic route to monomer was depicted in Scheme 1. Bromination of benzo[*c*][1,2,5]thiadiazole **1** was achieved with HBr and Br_2. Reduction product **3** of dibrominated benzothiadiazole **2** was condensed with terephthaldehyde in the presence of $ZrCl_4$ to yield electron deficient dibrominated benzimidazole unit **4**. Finally, target monomer **BIBA** was successfully synthesized by Stille coupling reaction of compound **4** with tributyl(thiophene-2-yl)stannane.

4.2. Electrochemical polymerization of the monomer

For electropolymerization, corresponding monomer was dissolved in dichloromethane (DCM) due to poor solubility, and mixed with ACN containing 0.1 M $LiClO_4/NaClO_4$ (1:1 mol) (DCM:ACN 5:95, v:v). Indium tin oxide coated glass slide, platinum and silver wires were used as the working, counter and pseudo reference electrodes, respectively. Silver wire pseudo reference electrode was calibrated against Fc/Fc^+ (0.3 V). In the first cycle monomer oxidation was revealed at 1.57 V. With following cycles a quasi-reversible oxidation and reduction couple for the polymer (PBIBA) were observed as shown in Fig. 1a.

4.3. Electrochemical and spectroelectrochemical properties

After the polymerization process, polymer coated ITO was washed with fresh ACN to remove unreacted monomer. Cyclic voltammogram of the polymer in a monomer free 0.1 M $LiClO_4/NaClO_4$ (1:1 mol) acetonitrile solution, revealed polymer redox couple at 1.43/1.18 V. HOMO level of the polymer was calculated as −6.1 eV. Although there are some examples of n-doping for benzimidazole polymers, for this derivative n-doping property could not been observed [21,24]. Using the optical band gap of the polymer, LUMO level was calculated as −4.18 eV (LUMO = Eg + HOMO)

In Fig. 1b relation between the scan rate and current density of the polymer was investigated and it was observed that the electrochemical processes are not diffusion-controlled according to modified Sevcik equation for non-diffusion-controlled electrochemical processes [25].

During spectroelectrochemical investigation of the polymer, stepwise oxidation was applied while the UV-vis–NIR spectra were recorded. By this method optical changes for the polymer in different applied potentials could be observed. Since HOMO level of donor unit in donor–acceptor–donor type polymers is high enough to make an energy transition to LUMO of the polymer, consecutively two π–π^* transitions were observed for these types of polymers in their neutral state. The polymer as a donor–acceptor–donor type revealed two π–π^* transitions at 347 nm and 478 nm, hence the polymer revealed yellowish-orange color in its neutral state and the optical band gap of the polymer was calculated as 1.92 eV from onset of the longer wavelength absorption (Fig. 2a). While the polymer was p-type doped, the intensity of two π–π^* transition peaks decreased and two new absorption peaks aroused at around 700 and 1280 nm. During the formation of the new bands, intensity of π–π^* transitions did not diminish completely. As a result a pale-green color was observed as the color of oxidized state. Also, a pale-gray color was observed along stepwise oxidation process. To report the colors of polymer in neutral and oxidized states, colorimetry studies were performed using CIE L*a*b* color space as shown in Fig. 2a.

For an electrochromic polymer, optical contrast, response time and stability in visible and NIR regions are important properties. In order to investigate these properties, polymer film were investigated at specific wavelengths between its neutral and oxidized states. For this purpose a square-wave potential step method was

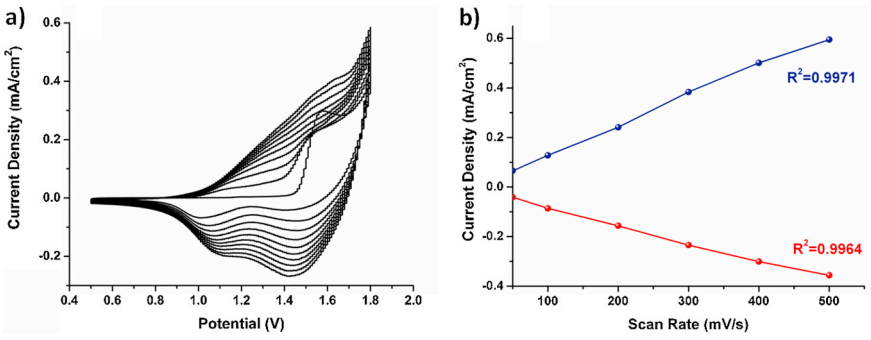

Fig. 1. (a) Cyclic voltammogram of monomer and (b) relation between current density and scan rate.

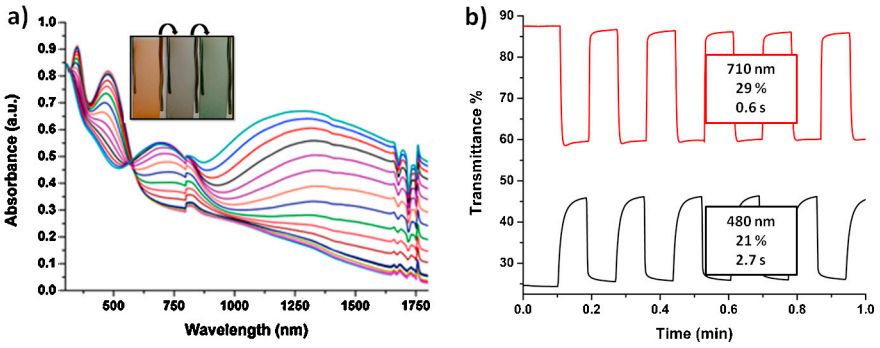

Fig. 2. (a) Spectra of the polymer during stepwise oxidation and (b) change of % transmittance and switching time of the polymer at 480 and 710 nm.

applied while optical spectroscopy was monitored. To obtain the switching time, the time difference between the fully reduced and oxidized states was calculated. The optical contrast for polymer was measured as the transmittance difference ($\Delta T\%$) between the neutral and oxidized states and calculated as 21% at 480 nm and 29% at 710 nm. The switching times were calculated as 0.6 s and 2.7 s at 480 and 710 nm, respectively and summarized in Fig. 2b.

4.4. Preparation of biosensor

To construct the desired biosensor, spectroscopic grade graphite rod electrode was polished on emery paper and washed with distilled water. After the rods were dried thoroughly, corresponding monomer was electropolymerized on graphite electrode in the presence of 0.1 M $LiClO_4/NaClO_4$ (1:1) in ACN/DCM (5:95, v:v) between the potential range 0.5 V and 1.8 V at a scan rate of 0.1 V s^{-1}. In biomolecule conjugation step, GOx (50 U in 5 μL 50 mM phosphate buffer, pH = 7.0) was immobilized with the help of GA (0.1% in 5 μL distilled water) on the polymer coated graphite electrode. During the immobilization step, imine bond formation was successfully achieved between free aldehyde groups of the polymer and free amine groups of the enzyme unit [26,27]. On the other hand, non-covalent interactions referred as π–π stacking was performed between unsaturated aromatic groups of polymer and enzyme [28,29]. In order to achieve strong attachment between functionalized polymer and biolayer without leaching the enzyme from the surface, both covalent binding and non-covalent interactions were successfully performed [30–32]. A schematic representation of fabricated biosensor is outlined in Scheme 2.

4.5. Optimization studies

Conducting polymers known as good transducers are also convenient bioconjugation matrices thanks to their easy structural modification for enzyme immobilization in biosensor applications [33]. During the immobilization process, film thickness (related with the scan number of electropolymerization) is of great importance in terms of morphology and biosensor response. A thick film on the bare graphite electrode due may hinder the electron transfer resulting in a longer response time. However, low polymer thickness affects the number of functional groups covalently attached to enzyme. Therefore some of the biomolecules on the polymer generated electrode may be unstabilized according to weak interaction with surface and easily leach during the amperometric measurements [34]. In order to determine desired polymer thickness, corresponding monomer was electropolymerized on different graphite rods with different scan numbers varying between 10 (0.35 mC, 7.75 nm) and 60 (20.76 mC, 46.52 nm) cycles. A certain amount of GOx was covalently attached on the surface using equal amounts of GA solution. Comparing the current responses with the scan numbers, polymers prepared with 20 (0.70 mC, 15.50 nm) and 40 (1.40 mC, 31.00 nm) scans have the highest responses. According to these results, 20 cycle polymerization (0.70 mC, 15.50 nm) was chosen as the optimum scan number for the desired biosensor.

To optimize the enzyme amount on the surface, working electrodes were coated with polymer using the optimum number of cycles. Then, new four sensors with different amounts of GOx (25.0 U, 50.0 U, 85.0 U and 120.0 U in 50 mM sodium acetate buffer) were constructed in the presence of glutaraldehyde. For the same glucose concentration highest response was observed with 50.0 U GOx.

Glutaraldehyde (GA) chemistry is a well known crosslinking technique to stabilize the biomolecule on the surface [35]. However, at high concentrations of GA, this bifunctional agent may affect enzyme activity resulting in a decrease in current response [36]. GA effect on the biosensor performance was investigated by measuring the current response in 50 mM sodium acetate buffer (pH = 5.5). For this purpose, different amounts of GA (0.05%, 0.1%,

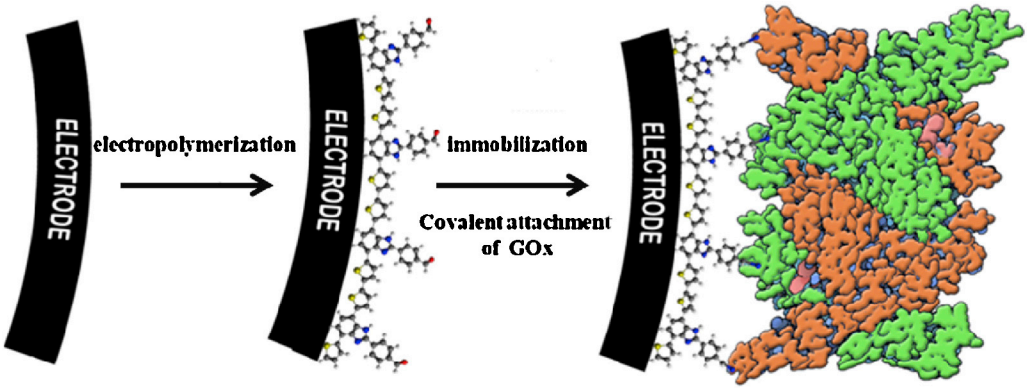

Scheme 2. Schematic representation of proposed biosensor construction.

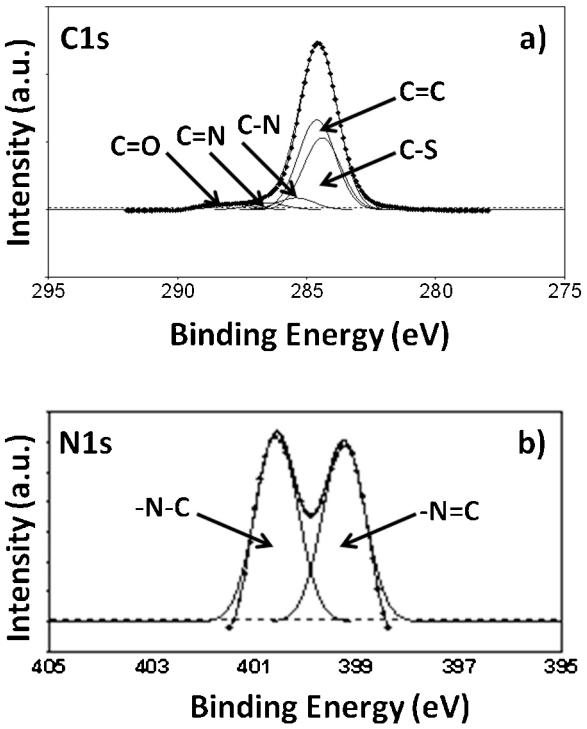

Fig. 3. (a) C1s and (b) N1s XPS spectra of the polymer surface.

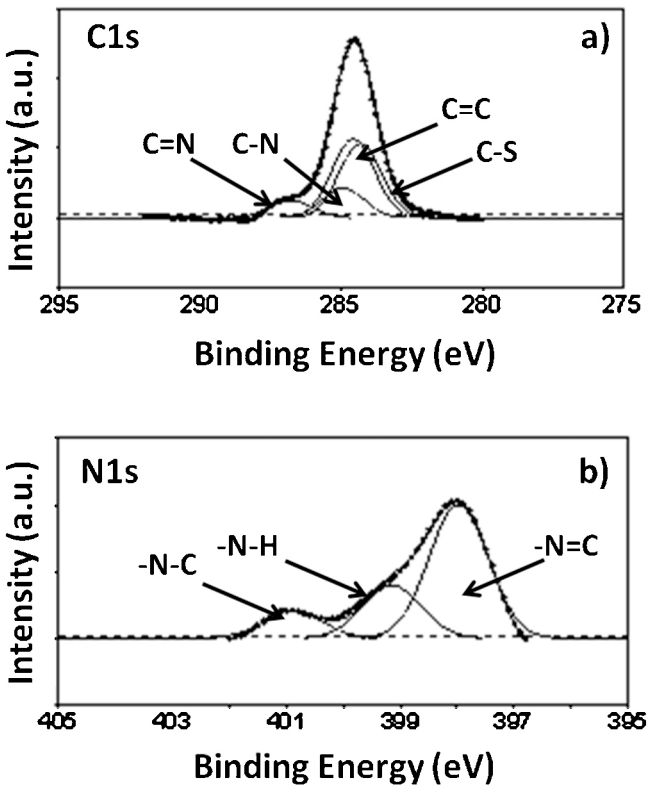

Fig. 4. (a) C1s and (b) N1s XPS spectra of protein immobilized onto the polymer surface.

0.5% and 1.2%) were used for each biosensor. As a result, 0.1% GA amount was found to be suitable for the highest current response in this study.

One of the essential parameters in biosensing studies is pH which causes enzyme denaturation in upper and lower values than the optimum one. To proceed with the measurements in optimum enzyme activity, working pH range should be determined. Optimization studies were carried out in different pH values varying between 4.5 and 6.5 (50 mM sodium acetate buffer at 4,5; 5.0; 5.5 and 50 mM phosphate buffer at 6.0; 6.5, 25 °C). According to the results in accordance with the current response, 5.5 was determined as the optimum pH value.

4.6. Surface characterization

Surface characterization was done via X-ray photoelectron spectroscopy (XPS). According to XPS results, the linkage formation between free amine groups of enzyme and aldehyde group of polymer was detected. The carbon and nitrogen signals were resolved using a fitting program as depicted in Figs. 3 and 4. Polymer exhibits signals related to aromatic bonds (aromatic carbons and C—S in thiophene unit at 284.6 eV and 284.4 eV, respectively), C=N group (285.4 eV), C—N and characteristic C=O group in aldehyde unit (286.5 eV and 287.8 eV, respectively) (Fig. 3a) [37,38]. It is possible to obtain information regarding this perfect attachment through investigating N1s spectra of the polymer. As illustrated in these spectra, the signals centered at 399.2 eV and 400.6 eV were assigned to =N-group and amine group in imidazole unit, respectively (Fig. 3b) [39].

In protein immobilized surface, absence of aldehyde signal and an increase in the intensity of C=N-signal prove bond formation between enzyme and polymer surface. Thus, the biomolecule was covalently attached to the polymer as expected (Fig. 4a). Hence relative increase in the intensity of N 1s of =N- and N—H peaks is attributed to new imine bonds and to new terminal amine groups of enzyme (Fig. 4b). Through these results, immobilization of biomolecule on polymer coated surface was successfully achieved.

4.7. Surface morphology

Surface characteristics were investigated using TEM. In Fig. 5 images show polymer coated surface (Fig. 5a) and GOx immobilized on polymer matrix (Fig. 5b). It is seen clearly that polymer was coated successfully with a uniform and ragged morphology on the surface. Due to small molecular size of the polymer, the surface features of this layer are naive than the one where biomolecule was attached. Contrary to polymer image, bulky and huge enzyme molecules crosslinked by GA completely covers the surface in a uniform and indented manner. Comparing these images, biomolecule and GA attached surface can be depicted as well-organized in terms of surface area to interact with the substrate.

4.8. Analytical characterization of constructed biosensor

The electroanalytic characterization of biosensor was performed using amperometric detection technique. Since oxygen consumption during the enzymatic redox reaction was achieved at −0.7 V constant potential, current responses versus time values were recorded at this potential. The calibration curve including varying glucose concentration versus current was established for optimum electrodes (Fig. 6). Kinetic parameters were calculated from the Lineweaver–Burk plot at constant temperature and pH 5.5 as summarized in Table 1. It was observed that optimum electrode has very low K_m^{app} value (0.94 mM) and high I_{max} (10.91 μA). These parameters reveal that enzyme has high affinity to its substrate. The linearity range of generated biosensor was determined as 0.02–1.2 mM with 0.998 correlation coefficient constant (Fig. 6).

Furthermore, shelf life and operational stability studies were carried out for the optimization of the biosensor (in 50 mM sodium

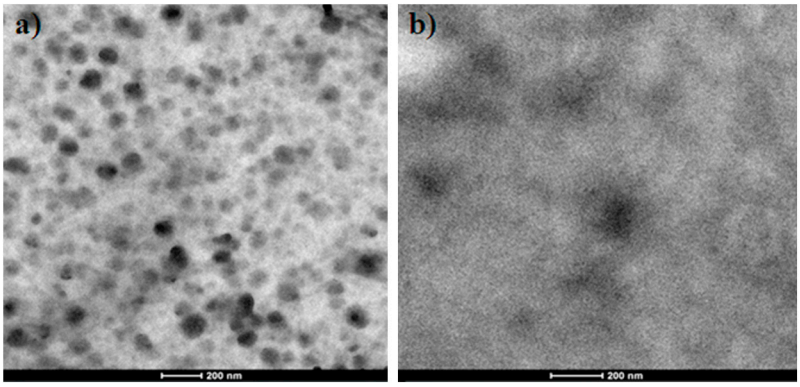

Fig. 5. TEM images of polymer (a) before and (b) after biomolecule immobilization under optimized conditions.

Table 1
Examples of glucose biosensors from literature.

Immobilization matrix	Limit of detection	K_m	Sensitivity ($\mu A/mM^{-1}$)	Refs.
PANI/PIP	0.01 mM	11.9 mM	12.20	[40]
Au/PDA/Fe_3O_4	6.50 μM	1.67 mM	NR	[41]
OOPPy/AuNPs	0.50 mM	NR	0.21	[9]
AuNP/(FcSH + Cyst)/PAMAM	0.6 mM	NR	NR	[42]
Poly(1,2-DAB)/CNT PBmodified	0.10 mM	NR	60.00	[43]
Poly(2-hydroxyethyl methacrylate)	25.00 μM	43.7 mM	0.47	[44]
1,10-Phenanthroline monohydrate	0.05 mM	0.64 mM	NR	[45]
Nafion–SWCNHs	6 μM	8.5 mM	1.06	[46]
PBIBA	2.29 μM	0.94 mM	6.74	TW

NR: not reported, TW: this work.

acetate buffer, pH 5.5, 25 °C, −0.7 V). To determine the operational stability, repeated measurements for 0.4 mM glucose at optimum ambient conditions were recorded where no decrease was observed for 61 consecutive measurements. Moreover, optimum sensor was daily tested for 0.4 mM glucose concentration. Between each sequential measurement, biosensor was stored at +4 °C in buffer solution to protect the enzyme from the environmental conditions. The shelf life of biosensor was examined for 28 days; no activity loss was observed.

Corresponding conducting polymer based biosensor has impressive kinetic parameters and very low LOD value with high sensitivity. Literature examples of polymer based glucose sensors were summarized in Table 1 to compare the properties of fabricated biosensor. According to these results, polyaniline and polyisoprene composite film based sensor exhibits low affinity to glucose [40]. In another example, magnetic Fe_3O_4 and gold modified polydopamine bionanoparticles were used as the immobilization matrix for GOx in the literature [41]. Measurable minimum glucose concentration for this biosensor was low and Michaelis–Menten constant, K_M^{app}, of this matrix revealed high affinity. 1,10-Phenanthroline monohydrate modified glassy carbon electrode based biosensor reveals lower K_M with a higher limit of detection [45]. Nafion–SWCNH composite film shows higher LOD and K_M values [46]. The designed immobilization matrix in this study depicts a high affinity to the substrate with a high sensitivity.

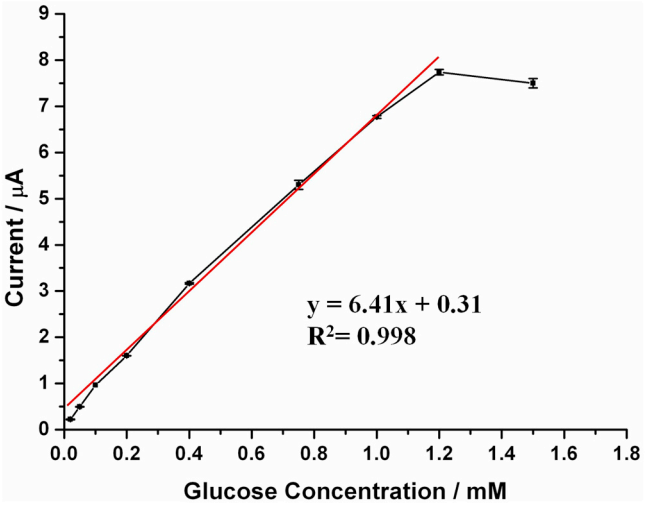

Fig. 6. Calibration curve for glucose (in 50 mM sodium acetate buffer solution, pH 5.5, 25 °C, −0.7 V). Error bars show the standard deviation (SD) for $n = 3$.

5. Conclusion

5.1. Sample applications

To obtain high accuracy results for sample applications, the response of a constructed biosensor in real sample containing interferents should be determined. In order to define the selectivity of biosensor to glucose, human blood samples containing several electroactive species such as ascorbic acid, oxalic acid and urea were examined. For this purpose, these agents were added into the buffer solution (50 mM sodium acetate buffer, pH 5.5, 25 °C) in different concentrations (0.1 M and 0.01 M) in the course of amperometric measurements at −0.7 V. However, no interfering effect was observed at given working conditions. Furthermore, corresponding biosensor was also tested for human blood serum samples. Preliminary detection of glucose amount in such samples was carried out with a reference method in a local health center. Then optimized electrode was tested using human blood serums instead of glucose. The glucose concentration was calculated in serum samples via amperometric measurements (50 mM sodium acetate buffer, pH 5.5, 25 °C, −0.7 V). All human blood sample experiments were approved by ethical committee. These results are compared

Table 2
Glucose analysis in real serum samples.

Sample	Hospital data (mM)	Designed biosensor (mM)	Relative error (%)
1	0.183	0.185	1.109
2	0.180	0.184	2.222
3	0.178	0.176	1.123
4	0.174	0.171	1.724
5	0.168	0.170	1.190
6	0.162	0.163	0.617
7	0.155	0.159	2.580

in Table 2. According to comparative study results, corresponding biosensor is appropriate for use in real samples.

6. Conclusions

In the present article a novel functionalized conducting polymer and its synthesis were reported. The biomolecule immobilization properties of functional conducting polymer were tested using GOx as the model enzyme. During this process, covalent and non-covalent attachment techniques were used to provide more robust interaction between biomolecule and polymer surface. Meanwhile, imine bond formation was successfully achieved for covalent attachment and characterized via XPS spectra. Through this robust interaction, the biosensor showed high electron affinity with low LOD value in good stability. Finally, the optimized biosensor was tested in human real blood serum samples with high accuracy values.

Acknowledgements

METU Central Laboratory is acknowledged for XPS analyses and TEM images. Also, METU Health Center is acknowledged for supplying blood serum samples.

References

[1] N. Gupta, S. Sharma, I.A. Mir, D. Kumar, J. Sci. Ind. Res. 65 (2006) 549.
[2] G. Nyström, A. Razaq, M. Strømme, L. Nyholm, A. Mihranyan, Nanoletters 9 (2009) 3635.
[3] C. Su, Y. Ye, L. Xu, C. Zhang, J. Mater. Chem. 22 (2012) 22658.
[4] A. Malinauskas, Synth. Met. 107 (1999) 75.
[5] H. Gao, J.B. He, Y. Wang, N. Deng, J. Power Sour. 205 (2012) 164.
[6] A. Balan, D. Baran, N.S. Sariciftci, L. Toppare, Sol. Energy Mat. Sol. C 94 (2010) 1797.
[7] S. Ozdemir, M. Sendur, G. Oktem, Ö. Doğan, L. Toppare, J. Mater. Chem. 22 (2012) 4687.
[8] L.P. Wang, W. Wang, L. Di, Y.N. Lu, J.Y. Wang, Colloid Surf. B 80 (2010) 72.
[9] B. Haghighi, M.A. Tabrizi, Colloid Surf. B 103 (2013) 566.
[10] Q.D. Ling, D.J. Liaw, C. Zhu, D.S.-H. Chan, E.T. Kang, K.G. Neoh, Prog. Polym. Sci. 33 (2008) 917.
[11] D. Pede, G. Serra, D.D. Rossi, Mater. Sci. Eng. 5 (1998) 289.
[12] L. Xia, Z. Wei, M. Wan, J. Colloid Interf. Sci. 341 (2010) 1.
[13] M. Yuksel, D.G. Colak, M. Akin, I. Cianga, M. Kukut, E.I. Medine, M. Can, S. Sakarya, P. Unak, S. Timur, Y. Yagci, Biomacromolecules 13 (2012) 2680.
[14] A.L. Goff, M. Holzinger, S. Cosnier, Analyst 136 (2011) 127.
[15] S. Cosnier, M. Holzinger, Chem. Soc. Rev. 40 (2011) 2146.
[16] N. Chauhan, J. Narang, C.S. Pundir, Analyst 136 (2011) 1938.
[17] H.A. Barker, R.D. Smyth, H. Weissbach, J.I. Toohey, J.N. Lad, B.E. Volcani, J. Biochem. 235 (1960) 480.
[18] K. Decamps, I.J. Joye, D. Haltrich, J. Nicholas, C.M. Courtin, J.A. Delcour, Food Chem. 131 (2012) 1485.
[19] E.P. Randviir, C.E. Banks, Anal. Methods 5 (2013) 1098.
[20] M. Yoshimoto, N. Takaki, M. Yamasaki, Colloid Surf. B 79 (2010) 403.
[21] H. Akpınar, A. Balan, D. Baran, E.K. Unver, L. Toppare, Polymer 51 (2010) 6123.
[22] K. Zhu, V.N. Vukotic, S.J. Loeb, Angew. Chem. Int. Ed. 51 (2012) 2168.
[23] S.S. Zhu, T.M. Swager, J. Am. Chem. Soc. 119 (1997) 12568.
[24] A.C. Ozercaglayan, M. Sendur, N. Akbasoglu, D.H. Apaydin, A. Cirpan, L. Toppare, Electrochim. Acta 67 (2012) 224.
[25] G. Sonmez, H. Meng, Q. Zhang, F. Wudl, Adv. Funct. Mater. 13 (2003) 726.
[26] X. Xu, Y. Feng, J. Li, F. Li, H. Yu, Biosens. Bioelectron. 25 (2010) 2324.
[27] R.E. Fernandez, E. Bhattacharya, A. Chadha, Appl. Surf. Sci. 254 (2008) 4512.
[28] U. Lange, N.V. Roznyatovskaya, V.M. Mirsky, Anal. Chim. Acta 614 (2008) 1.
[29] S. Grimme, Angew. Chem. Int. Ed. 47 (2008) 3430.
[30] C.G. Palivan, O.F. Onaca, M. Delcea, F. Itel, W. Meier, Chem. Soc. Rev. 41 (2012) 2800.
[31] M. Shi, J. Lu, M.S. Soichet, J. Mater. Chem. 19 (2009) 5485.
[32] F.B. Emre, F. Ekiz, A. Balan, S. Emre, S. Timur, L. Toppare, Sensor Actuat. B 158 (2011) 117.
[33] S. Demirci, F.B. Emre, F. Ekiz, F. Oğuzkaya, S. Timur, C. Tanyeli, L. Toppare, Analyst 137 (2012) 4254.
[34] S. Cosnier, Appl. Biochem. Biotechnol. 89 (2000) 127.
[35] M.D. Gouda, M.A. Kumar, M.S. Thakur, N.G. Karanth, Biosens. Bioelectron. 17 (2002) 503.
[36] V. Singh, M. Zharnikov, A. Gulino, T. Gupta, J. Mater. Chem. 21 (2011) 10602.
[37] Y. Wang, Z. Shi, J. Fang, H. Xu, J. Yin, Carbon 49 (2011) 1199.
[38] W. Ai, W. Zhou, Z. Du, Y. Du, H. Zhang, X. Jia, L. Xie, M. Yi, T. Yu, W. Huang, J. Mat. Chem. 22 (2012) 23439.
[39] M.Y. Hua, H.C. Chen, R.Y. Tsai, Y.C. Lin, L. Wang, Anal. Chim. Acta 693 (2011) 114.
[40] H. Xue, Z. Shen, Y. Li, Synth. Met. 124 (2001) 345.
[41] H.P. Peng, R.P. Liang, L. Zhang, J.D. Qui, Biosens. Bioelectron. 42 (2013) 293.
[42] M. Karadag, C. Geyik, D.O. Demirkol, F.N. Ertas, S. Timur, Mat. Sci. Eng. C 33 (2013) 634.
[43] A. Curulli, F. Valentini, S. Orlanduci, M.L. Terranova, G. Palleschi, Biosens. Bioelectron. 20 (2004) 1223.
[44] S. Brahim, D. Narinesingh, A.G. Elie, Biosens. Bioelectron. 17 (2002) 53.
[45] Y. Oztekin, A. Ramanaviciene, Z. Yazicigil, A.O. Solak, A. Ramanavicius, Biosens. Bioelectron. 26 (2011) 2541.
[46] X. Liu, L. Shi, W. Niu, H. Li, G. Xu, Biosens. Bioelectron. 23 (2008) 1887.